Franck-Condon simulation, including anharmonicity, of the photodetachment spectrum of P_2H^-: Restricted-spin coupled-cluster single-double plus perturbative triple and unrestricted-spin coupled-cluster single-double plus perturbative triple -F12x potential energy functions of P_2H and P_2H^-

Daniel K. W. Mok,[1,a)] Edmond P. F. Lee,[1,2,a)] Foo-tim Chau,[1] and John M. Dyke[2]
[1]*Department of Applied Biology and Chemical Technology, The Hong Kong Polytechnic University, Hung Hom, Hong Kong*
[2]*School of Chemistry, University of Southampton, Highfield, Southampton SO17 1BJ, United Kingdom*

(Received 28 June 2011; accepted 29 August 2011; published online 30 September 2011)

Geometry optimization and harmonic vibrational frequency calculations have been carried out on the $\tilde{X}^2A'$ state of P_2H and the $\tilde{X}^1A'$ state of P_2H^- using the restricted-spin coupled-cluster single-double plus perturbative triple excitation [RCCSD(T)] and explicitly correlated unrestricted-spin coupled-cluster single-double plus perturbative triple excitation [UCCSD(T)-F12x] methods. For RCCSD(T) calculations, basis sets of up to the augmented correlation-consistent polarized valence quintuple-zeta (aug-cc-pV5Z) quality were employed, and contributions from extrapolation to the complete basis set limit and from core correlation of the P $2s^22p^6$ electrons were also included. For UCCSD(T)-F12x calculations, different atomic orbital basis sets of triple-zeta quality with different associated complementary auxiliary basis sets and different geminal Slater exponents were used. When the P $2s^22p^6$ core electrons were correlated in these F12x calculations, appropriate core-valence basis sets were employed. In addition, potential energy functions (PEFs) of the $\tilde{X}^2A'$ state of P_2H and the $\tilde{X}^1A'$ state of P_2H^- were computed at different RCCSD(T) and UCCSD(T)-F12x levels, and were used in variational calculations of anharmonic vibrational wavefunctions, which were then utilized to calculate Franck-Condon factors (FCFs) between these two states, employing a method which includes allowance for anharmonicity and Duschinsky rotation. The photodetachment spectrum of P_2H^- was then simulated using the computed FCFs. Simulated spectra obtained using the RCCSD(T)/aug-cc-pV5Z and UCCSD(T)-F12x(x = a or b)/aug-cc-pCVTZ PEFs are compared and found to be essentially identical. Based on the computed FCFs, a more detailed assignment of the observed vibrational structure than previously reported, which includes "hot bands," has been proposed. Comparison between simulated and available experimental spectra has been made, and the currently most reliable sets of equilibrium geometrical parameters for P_2H and its anion have been derived. The photodetachment spectrum of P_2D, yet to be recorded, has also been simulated.
 [doi:10.1063/1.3640037]

INTRODUCTION

Recently, two high-level *ab initio* studies have been reported on the diphosphenyl radical (P_2H) and related species. One of them, published in 2006, was on the investigation of hydrogen bridging in X_2H compounds, where X = Al, Si, P, and S.[1] Both P_2H and its anion were considered with a view to identifying suitable X_2H and X_2H^- type species, which may prevent uniform layer deposition in a chemical vapor deposition process through the scavenging of reactant molecules in the semiconductor industry.[1] The restricted-spin coupled-cluster single-double plus perturbative triple excitation [RCCSD(T)] method, and the density functional theory (DFT) method with various functionals, were employed. The highest level of calculation performed was RCCSD(T) with the augmented correlation-consistent polarized valence quadruple-zeta (aug-cc-pVQZ) basis set. The second study, published in 2007, was on the heats of formation of various P_nH_m molecules, as possible chemical hydrogen storage systems.[2] P_2H was considered because it is a product from the PH cleavage of P_2H_4. The highest level of calculations used in this investigation[2] to obtain the equilibrium geometry and harmonic vibrational frequencies of P_2H, were RCCSD(T)/aug-cc-pV(T+d)Z. Further single energy calculations at the RCCSD(T)/aug-cc-pV(Q+d)Z level were also carried out, for extrapolation to the complete basis set (CBS) limit, in order to obtain more accurate heat of formation. In summary, these two computational studies[1,2] on P_2H demonstrate recent interest in this radical and its relevance to a number of areas.

Prior to the computational studies[1,2] described above, the 351.1 nm ($h\nu$ = 3.531 eV) laser negative-ion photoelectron spectrum of P_2H^- was reported in 2005.[3] To our knowledge, this is the only spectroscopic study available on

[a)]Authors to whom correspondence should be addressed. Electronic addresses: bcdaniel@polyu.edu.hk and epl@soton.ac.uk.

P_2H. In this photodetachment study,[3] in order to assist assignment of the observed photodetachmant band, DFT calculations at the B3LYP/aug-cc-pVTZ level were performed to obtain optimized geometries and harmonic vibrational frequencies, and single energy coupled-cluster single-double plus perturbative triple CCSD(T)/aug-cc-pVTZ calculations were used to evaluate the electron affinity of P_2H. In addition, Franck-Condon factors (FCFs) were calculated within a harmonic-oscillator model, which included Duschinsky rotation, using normal coordinate vectors from the B3LYP/aug-cc-p-VTZ frequency calculations, in order to simulate the vibrational structure in the photodetachment spectrum. Based on the results of the *ab initio* and FCF calculations, the observed vibrational structure with a major progression of 630 ± 20 cm^{-1} and a minor progression of 2160 ± 30 cm^{-1} was assigned to the PPH bending mode (ν_2') and the PH stretching mode (ν_1') of P_2H, respectively. Although no vibrational structure due to the PP stretching mode (ν_3') was identified in the observed spectrum, using the Franck-Condon intensities to fit the displacements in the other two modes, estimates of increases of 0.023 Å, 0.068 Å, and 8° in the PP and PH distances, and the PPH angle, respectively, from the neutral to the anion were obtained via the iterative Franck-Condon analysis (IFCA; *vide infra*) procedure.[3] Subsequent to this experimental photodetachment study[3] on P_2H^-, a combined *ab initio*/FCF study on the photodetachment spectrum of P_2H^- was published in 2006.[4] DFT and *ab initio* calculations were performed, with the highest level being CCSD/6-311+G(2*d*,*p*). The FCF calculations carried out in Ref. 4 were similar to those of Ref. 3, i.e., they used the harmonic oscillator model. In Ref. 4, the geometrical parameters obtained for P_2H^- were $r_e(PH) = 1.503 \pm 0.001$ Å and $\theta_e(PPH) = 106.3 \pm 0.2°$. However, in the IFCA procedures carried out in both Refs. 3 and 4, the geometry of P_2H was fixed to the computed B3LYP/aug-cc-pVTZ and B3LYP/6-311+G(2*d*,*p*) geometries, respectively, because experimental geometrical parameters of P_2H were unavailable at the time (and even now), and the geometrical parameters of the anion were varied until the best match between the simulated and observed vibrational structure was obtained. Clearly, this is far from the ideal as the B3LYP geometries of P_2H used in the IFCA procedures of both Refs. 3 and 4 differ significantly from available, later computed, higher level CCSD(T) geometries[1,2] (for example, B3LYP θ_e values[3,4] of ~98° c.f. RCCSD(T) values[1,2] of ~97°; *vide infra*). In addition, in both cases,[3,4] FCFs were computed within the harmonic oscillator model, although it is expected that contributions from anharmonicity will be considerable, at least for the PH stretching (ω_1) mode of P_2H and P_2H^-. Indeed, the large differences of ~140 cm^{-1} between available computed harmonic ω_1 values[1–4] of ~2300 cm^{-1} and the observed fundamental ν_1 value of 2160 ± 30 cm^{-1} for P_2H from the experimental photodetachment spectrum[3] clearly show the importance of including anharmonicity in the theoretical model to be employed to describe the system. In view of these inadequacies in previous studies, we propose to carry out state-of-the-art *ab initio* calculations on P_2H and its anion in order to obtain their most reliable theoretical geometrical parameters and to perform FCF calculations, which include anharmonicity.

In addition to the conventional CCSD(T)/CBS approach using correlation consistent basis sets, which may be currently considered as the gold standard of quantum chemistry,[5–7] the recently reported, explicitly correlated UCCSD(T)-F12x (x = a or b) methods,[8] which correct the lack of derivative discontinuity (cusp) in standard wavefunctions,[9,10] have also been employed. The use of the UCCSD(T)-F12x method follows our recently published works on AsX_2 (X = H, F, or Cl), and their ions,[11–13] where Franck-Condon spectral simulations including allowance for anharmonicity were carried out on the $\tilde{A}(0,0,0)$-$\tilde{X}$ SVL emission spectrum of AsH_2,[11] the photoelectron spectra of AsF_2 and $AsCl_2$, and the photodetachment spectra of AsF_2^- and $AsCl_2^-$,[12,13] using UCCSD(T)-F12x potential energy functions (PEFs). In these studies,[11–13] it was concluded that the explicitly correlated method, UCCSD(T)-F12x, could be used to generate reliable PEFs *in lieu* of conventional correlated methods, such as RCCSD(T), at a considerably reduced cost. Specifically, simulated spectra obtained using RCCSD(T)/aug-cc-pCV5Z and RHF/UCCSD(T)-F12a/aug-cc-pCVTZ PEFs are essentially identical (see Refs. 11 and 12), indicating that with a smaller basis set, the F12 method has produced comparable results to those of the RCCSD(T) method with a larger basis set.

THEORETICAL METHODS AND COMPUTATIONAL DETAILS

Geometry optimization and harmonic vibrational frequency calculations were carried out on the $\tilde{X}^2A'$ state of P_2H and the $\tilde{X}^1A'$ state of P_2H^-, employing the RCCSD(T) (Ref. 14) and UCCSD(T)-F12x (Ref. 8) methods, as implemented in the MOLPRO suite of programs.[15] The various basis sets,[16–28] frozen cores, and the geminal Slater exponent (β in F12 calculations; *vide infra*) used are summarized in Table I (see footnotes of Table I and the MOLPRO online manual[27]). For RCCSD(T) calculations, the largest basis set used is the aug-cc-pwCV5Z basis set,[19] which consists of 514 contracted Gaussian functions for P_2H. Extrapolations of optimized geometrical parameters and computed relative electronic energies to the CBS limit were carried out employing the two point $1/X^3$ extrapolation formula[29–31] with the computed RCCSD(T) values, using the aug-cc-pwCVQZ (basis A) and aug-cc-pwCV5Z (basis B) basis sets, which also include P $2s^2 2p^6$ core correlation. For UCCSD(T)-F12x calculations, the scaled perturbative triples obtained by a simple scaling factor, $\Delta E(T_{sc}) = \Delta E(T) \times E_{corr}^{MP2\text{-}F12}/E_{corr}^{MP2}$ (i.e., the ratio between the computed correlation energies obtained at the MP2 and MP2-F12 levels; see Refs. 8 and 27), have been used throughout. In general, the choices of the various AO (atomic orbital), RI [resolution of the identity or associated complementary auxiliary basis sets (CABS) for RI approximations], and DF (density fitting) basis sets, and the corresponding β values [in the nonlinear correlation factor, $\hat{F}(r_{12}) = -(1/\beta)\exp(-\beta r_{12})$, used in the explicitly correlated wavefunction], used in the F12 calculations have followed recommendations of Refs. 8 and/or 21.

The PEFs of the two electronic states involved, the corresponding anharmonic vibrational wavefunctions and FCFs were computed as described previously.[32–34] Briefly, the PEFs

TABLE I. Basis sets and the corresponding frozen cores used in the present study.[a]

Basis	AO[b]	RI	DF	Core[c]
A2	AV(Q+*d*)Z; AVQZ (224)	...	...	P 1*s*2*s*2*p*
B1	AV(5+d)Z; AV5Z (352)	...	...	P 1*s*2*s*2*p*
A1	AwCVQZ; AVQZ (314)	...	...	P 1*s*2*s*2*p*
A	AwCVQZ; AVQZ (314)	...	...	P 1*s*
B	AwCV5Z; AV5Z (514)	...	...	P 1*s*
C[d]	VTZ-F12 (142)	AVTZ/JKFIT (338)	AVTZ/MP2FIT (340)	P 1*s*2*s*2*p*
D[d,e]	VTZ-F12 (142)	AVTZ_optri (185)	AVTZ/MP2FIT (340)	P 1*s*2*s*2*p*
E[f,g]	ACVTZ; AVTZ (173)	CVTZ-F12_opt (263)	AVTZ/MP2FIT (340)	P 1*s*

[a]All basis sets used belong to the polarized correlation-consistent (p-cc) type (Refs. 16–19 with A, C, V, and wC denoting augmented, core, valence, and energy-weighed core, respectively. While F12 denotes basis sets (Refs. 20 and 21) optimized for F12 calculations, opt or optri denotes RI (resolution of the identity) basis sets (Refs. 21–23) optimized for F12 calculations with the corresponding F12 AO basis sets. The numbers in parentheses are the total numbers of contracted Gaussian functions for P_2H used in the calculations. RI and DF (Refs. 21 and 24–26) basis sets were employed only in F12 calculations.

[b]When two entries appear, the first basis set is for P, while the second, for H; otherwise, basis sets of the same quality were used for both P and H.

[c]Only core electrons in these inner shells were frozen in the correlation calculations.

[d]For the nonlinear correlation factor, $\hat{F}(r_{12}) = -(1/\beta)\exp(-\beta r_{12})$, used in the explicitly correlated wavefunction, the default value (used in MOLPRO (Ref. 27)) for the geminal Slater exponent, β, of 1.0 was used in valence F12 calculations employing these basis sets (see also Ref. 21). The VTZ−F12, AVTZ/JKFIT, and AVTZ/MP2FIT basis sets are from the MOLPRO basis set library (Ref. 27).

[e]The AVTZ_optri basis sets used for P and H are from the EMSL website (Ref. 28).

[f]When P $2s^2 2p^6$ electrons were included explicitly in the F12 correlation treatment, the β value was set to 1.4 for all electrons (i.e., both valence and core), as recommended in Ref. 21.

[g]The CVTZ−F12_opt basis set from the basis set library website of MOLPRO (Ref. 27) was used for P, while the AVTZ_optri basis set (see footnote e) was used for H.

have the form of the polynomial,

$$V = \sum_{ijk} C_{ijk}(S_1)^i(S_2)^j(S_3)^k + V_{eqm}.$$

S_2 is the bending coordinate of Carter and Handy,[35] $S_2 = \Delta\theta + \alpha\Delta\theta^2 + \beta\Delta\theta^3$, where $\Delta\theta$ is the displacement of the bond angle from the equilibrium value, $(\theta–\theta_e)$. S_1 and S_3 are the displacements of the HP and PP bond lengths from the equilibrium values, $(r–r_e)$, respectively. Energy scans over all three internal coordinates (PP, PH, and θ) from the equilibrium positions of P_2H and P_2H^- were carried out at the RCCSD(T)/B1, UCCSD(T)-F12a/E, and UCCSD(T)-F12b/E levels, and the computed total electronic energies were used for PEF fittings. The root-mean-square (rms) deviations between the fitted PEFs and the computed *ab initio* energies are between 10.3 and 16.6 cm^{-1}.

Variational calculations, which employed the rovibronic Hamiltonian of Watson[36] for a nonlinear molecule, were carried out to obtain the anharmonic vibrational wavefunctions and energies. The anharmonic vibrational wavefunctions were expressed as linear combinations of harmonic oscillator functions (see Ref. 33). In the simulation of the photodetachment band of P_2H^-, vibrational components were simulated using Gaussian functions with a full width at half maximum (FWHM) of 5 meV. The relative intensity of each vibrational component in a simulated spectrum is the corresponding computed anharmonic FCF (with the FCF of the strongest vibrational component or the band maximum set to 100 in the simulated spectrum). The experimental EA_0 value of 1.514 eV from Ref. 3 has been used in all simulated spectra in order to facilitate a direct comparison between the simulated and observed vibrational structure. Vibrational "hot bands" (photodetachment bands arising from excited vibrational levels of the anion) were considered in the FCF calculations, assuming various Boltzmann vibrational temperatures, because "hot bands" had been identified in the experimental vibrational structure,[3] though no discussion of them in the photodetachment spectrum of P_2H^- was given in Ref. 3 and "hot bands" were ignored in Ref. 4. The IFCA procedure (see also Ref. 37), mentioned above and carried out in Refs. 3 and 4, has also been carried out in the present study. However, in contrast to previous studies,[3,4] which had employed B3LYP geometries for P_2H, the IFCA procedure carried out in the present study was based on the RCCSD(T)/CBS geometries of the two states (*vide infra*), which are currently the most reliable theoretical geometries for P_2H and P_2H^-.

RESULTS AND DISCUSSIONS

Optimized geometrical parameters

Optimized geometrical parameters of P_2H and its anion obtained in the present work at different levels of calculation are summarized in Tables II and III, respectively, together with available theoretical and experimental values for comparison. Based on the results from the series of RCCSD(T) calculations performed here on P_2H, as given in Table II, while basis size (from QZ to 5Z quality) effects reduce the computed PP bond lengths (r_e) of P_2H by [0.0029(without core); 0.0021(with core)] Å, core correlation (without and with P $2s^2 2p^6$ correlation) effects also reduce them by [0.0087(QZ); 0.0079(5Z)] Å, respectively. For computed PH bond lengths of P_2H, while basis size effects are negligibly small (±0.0002 Å), core effects reduce their values by [0.0035(QZ); 0.0031(5Z)] Å. Regarding computed PPH bond angles, θ, both basis set and core correlation effects can be considered as insignificantly small (<0.1°). The best

TABLE II. Computed equilibrium geometrical parameters (bond distances in Å and bond angles in degrees) and vibrational frequencies (ω and [ν] values in cm^{-1}) of P_2H obtained at different levels of calculations.

Methods	PP	PH	θ	ω_1(PH), $\omega_2(\theta)$, ω_3(PP)	Reference[a]
RCCSD(T)/A2	2.0085	1.4283	97.03	2306.0, 649.9, 607.9	PW
RCCSD(T)/B1	2.0056	1.4281	97.08	2304.3, 649.5, 608.8	PW
RCCSD(T)/B1 PEF	2.0060	1.4274	96.98	2307.1, 665.5, 609.7	PW
				[2194.5, 651.3, 601.6]	
RCCSD(T)/A1	2.0070	1.4278	97.06		PW
RCCSD(T)/A	1.9998	1.4248	97.01		PW
RCCSD(T)/B	1.9977	1.4250	97.03		PW
RCCSD(T)/CBS[b]	1.9955(22)	1.4252(2)	97.05(2)		PW
UCCSD(T)-F12b/C	2.0064	1.4287	97.16		PW
UCCSD(T)-F12b/D	2.0060	1.4288	97.19	2301.9, 659.8, 608.0	PW
UCCSD(T)-F12b/E	2.0009	1.4257	97.12	2304.2, 659.5, 608.6	PW
UCCSD(T)-F12a/E PEF	2.0005	1.4260	97.12	2299.3, 655.2, 600.7	PW
				[2191.5, 647.2, 595.8]	
UCCSD(T)-F12b/E PEF	2.0008	1.4261	97.10	2299.0,655.1, 600.3	PW
				[2190.9, 647.2, 595.4	
B3LYP/AVTZ	2.007	1.435	98	2267, 666, 611	3
B3LYP/6-311G(2*d*,*p*)	2.009	1.432	98.1	2260, 669, 608	4
MP2/6-311+G(2*d*,*p*)	2.049	1.419	96.1	2396.9, 689.2, 632.3	4
QCISD/6-311+G(2*d*,*p*)	2.032	1.423	97.5	2346.6, 684.7, 610.0	4
CCSD(6-311+G(2*d*,*p*)	2.031	1.422	97.2	2350.4, 690.8, 609.6	4
B3LYP/DZP++	2.014	1.437	98.7	2264, 673, 604	1
RCCSD(T)/AVQZ	2.012	1.430	97.0	2305, 663, 610	1
RCCSD(T)/AVTZ	2.027	1.432	97.4	2296.8, 657.1, 598.8	2
RCCSD(T)/AV(T+*d*)Z	2.020	1.429	96.8		2
Photodetachment				[2160(30), 630(20), −]	3
IFCA[c]	1.9955	1.4252	96.47		PW

[a]PW for present work.

[b]Extrapolation to the complete basis set (CBS) limit using the $1/X^3$ formula with the RCCSD(T)/A and RCCSD(T)/B values (see text). The estimated uncertainty is the difference between the RCCSD(T)/CBS and RCCSD(T)/B values.

[c]The geometrical parameters of the two electronic states were fixed to the RCCSD(T)/CBS values, except for the bond angle of the neutral, which was set to 96.47° (see text).

estimates of the equilibrium geometrical parameters of P_2H at the RCCSD(T)/CBS level are $r_e(PP) = 1.9955 \pm 0.0022$ Å, $r_e(PH) = 1.4252 \pm 0.0002$ Å, and $\theta(PPH) = 97.05 \pm 0.02°$ (see footnote b of Table II for the estimated uncertainties), and are clearly the most reliable theoretical values currently available (see Table II).

For P_2H^-, basis size and core correlation effects on the computed geometrical parameters behave in a very similar way to P_2H (see Tables II and III) and hence will not be discussed again. The best estimates at the RCCSD(T)/CBS level are $r_e(PP) = 2.0142 \pm 0.0024$ Å, $r_e(PH) = 1.4531 \pm 0.0003$ Å, and $\theta(PPH) = 105.72 \pm 0.01°$ (see footnote b of Table III for the estimated uncertainties), and are the currently most reliable theoretical values.

Considering the UCCSD(T)-F12x results as shown in Tables II and III, for both P_2H and its anion, the differences between using bases C and D (see Table I) are negligibly small. This indicates that, as far as the RI basis sets used are concerned, the considerably smaller AVTZ_optri basis set works as well as the considerably larger AVTZ/JKFIT basis set (see Table I), and hence these smaller RI optimized basis sets are strongly recommended to be used in future F12 calculations instead of the larger JKFIT-type basis sets. With the UCCSD(T)-F12b/E results for both P_2H and its anion, core correlation effects (cf. results from using bases C and D, where the P $2s^22p^6$ core electrons were not correlated) can be considered as generally behaving similar to those with RCCSD(T) calculations discussed above. When the computed UCCSD(T)-F12b/E geometrical parameters of both P_2H and its anion are compared with the corresponding RCCSD(T)/B and RCCSD(T)/CBS values, it is pleasing that the largest differences, which are with the PP bond length, are <0.0029 and <0.0055 Å, respectively. The agreement in the computed bond angles is generally within 0.1°. It should be noted that a single energy calculation on P_2H at the RCCSD(T)/B level takes >19.5 times CPU time more than that at the UCCSD(T)-F12x/E level. The equilibrium geometries of P_2H and its anion will be further discussed, when the IFCA procedure is considered below.

COMPUTED VIBRATIONAL FREQUENCIES

First, from the results shown in Tables II and III, it can be seen that the ranges of computed harmonic vibrational frequencies for all three vibrational modes of both P_2H and P_2H^- obtained at different RCCSD(T) and UCCSD(T)-F12b levels in the present study are within ~10 cm^{-1}. In this connection, a reasonable estimate for the maximum uncertainties

TABLE III. Computed equilibrium geometrical parameters (bond distances in Å and bond angles in degrees) and vibrational frequencies (ω and [ν] values in cm^{-1}) of P_2H^- obtained at different levels of calculations.

Methods	PP	PH	θ	ω_1(PH), $\omega_2(\theta)$, ω_3(PP)	Reference[a]
RCCSD(T)/A2	2.0274	1.4566	105.64	2054.9, 815.2, 599.8	PW
RCCSD(T)/B1	2.0247	1.4566	105.68	2053.2, 816.4, 601.8	PW
RCCSD(T)/B1 PEF	2.0253	1.4556	105.44	2057.4, 823.4, 600.2	PW
				[1920.7, 801.1, 596.4]	
RCCSD(T)/A1	2.0259	1.4562	105.67		PW
RCCSD(T)/A	2.0189	1.4538	105.70	2054.9, 818.9, 604.0	PW
RCCSD(T)/B	2.0166	1.4534	105.71		PW
RCCSD(T)/CBS[b]	2.0142(24)	1.4531(3)	105.72(1)		PW
UCCSD(T)-F12b/C	2.0239	1.4572	105.80		PW
UCCSD(T)-F12b/D	2.0238	1.4573	105.82	2047.9, 816.2, 601.9	PW
UCCSD(T)-F12b/E	2.0194	1.4546	105.70	2045.7, 815.0, 601.5	PW
UCCSD(T)-F12a/E PEF	2.0191	1.4546	105.74	2036.2, 815.5, 600.8	PW
				[1895.3, 797.6, 596.2]	
UCCSD(T)-F12b/E PEF	2.0192	1.4547	105.76	2035.2, 815.4, 599.2	PW
				[1893.7, 797.6, 594.7]	
B3LYP/6-311G(2*d*,*p*)	2.038	1.464	105.7	1994, 829, 588	4
MP2/6−311+G(2*d*,*p*)	2.040	1.444	106.1	2153.3, 835.9,597.0	4
QCISD/6−311+G(2*d*,*p*)	2.047	1.447	105.7	2118.2, 840.5, 586.1	4
CCSD/6−311+G(2*d*,*p*)	2.045	1.446	105.6	2126.1, 842.7, 592.3	4
B3LYP/DZP++	2.037	1.471	106.4		1
BLYP/DZP++				1988, 824, 587	1
RCCSD(T)/AVQZ	2.032	1.458	105.5	2050, 812, 597	1
IFCA[c]	2.030	1.503	106	−, [814], −	3
IFCA[d]		1.503(1)	106.3(2)		4
IFCA[e]	2.0142	1.4531	106.3		PW

[a]PW for present work.
[b]Extrapolation to the complete basis set (CBS) limit using the $1/X^3$ formula with the RCCSD(T)/A and RCCSD(T)/B values (see text). The estimated uncertainty is the difference between the RCCSD(T)/CBS and RCCSD(T)/B values.
[c]The geometrical parameters of the anion were derived from fitting computed Franck-Condon factors to the observed vibrational structure using the B3LYP/AVTZ geometry of the neutral; see original work for detail. The ν_2 value is estimated from the observed hot band in the experimental photodetachment spectrum of Ref. 3.
[d]Employing the B3LYP/6-311G(2*d*,*p*) geometry of the neutral to obtain the geometry of the anion; see original work for detail.
[e]The geometrical parameters of the two electronic states were fixed to the RCCSD(T)/CBS values, except for the bond angle of the anion which was set to 106.3° (see text).

associated with the computed vibrational frequencies reported here is approximately ± 10 cm^{-1}. Second, computed fundamental vibrational frequencies of both P_2H and P_2H^- are reported in the present study for the first time, and they are generally smaller than the corresponding harmonic values, as expected. In particular, the computed fundamental frequencies of the PH stretching modes of P_2H and P_2H^- are smaller than the corresponding harmonic values by ∼110 and 140 cm^{-1}, respectively, showing considerable contributions from anharmonicity to the PH stretching mode of both P_2H and its anion. Third, comparing computed fundamental frequencies of P_2H reported here with available experimental values obtained from the photodetachment spectrum of P_2H^-,[3] it is pleasing that the agreement is within the combined theoretical and experimental uncertainties of ±40 and ±30 cm^{-1} for the ν_1' (PH) and ν_2' (θ) modes, respectively. Finally, although no vibrational frequency of P_2H was reported in Ref. 3, a vibrational component in the "hot band" of the photodetachment spectrum at an electron binding energy of ∼1.42 eV was assigned to $2_1{}^0$ in Ref. 4. From the "hot band" in the published photodetachment spectrum of Ref. 3, an experimental ν_2'' (θ) value for P_2H^- can be estimated to be ∼814 cm^{-1}, which agrees very well with our computed fundamental values of between ∼798 [UCCSD(T)-F12x/E] and 801 [RCCSD(T)/B1] cm^{-1} (see Table III). The assignment of the vibrational structure in the experimental photodetachment spectrum will be further discussed, when the simulated spectra are considered later.

Computed electron affinities of P_2H

Computed electron affinities (EA) obtained at different levels of calculations are summarized in Table IV. Based on the RCCSD(T) results of the present study, it can be seen that while core contributions reduce computed EA values by ∼0.010 eV, basis size contributions increase computed EA values by ∼0.015 eV. The best RCCSD(T)/CBS value, which has also included core contributions, is 1.536 ± 0.014 eV (see footnote b of Table IV). Including zero-point energy (ZPE) corrections, the best EA_0 value is 1.543 eV. Comparing this best theoretical value with the experimental value of 1.514 ± 0.010 eV from the photodetachment spectrum of P_2H^-,[3] the difference of 0.029 eV (0.67 kcal $mole^{-1}$) is slightly larger than the combined theoretical and experimental uncertainty of ± 0.024 eV, suggesting that the $1/X^3$ extrapolation method

TABLE IV. Computed electron affinities (EA [EA_0] in eV) of P_2H obtained at different levels of calculations.

Method	EA	Reference[a]
RCCSD(T)/A2	1.516 [1.522]	PW
RCCSD(T)/B1	1.531 [1.537]	PW
RCCSD(T)/A1	1.517	PW
RCCSD(T)/A	1.507	PW
RCCSD(T)/B	1.522	PW
RCCSD(T)/CBS[b]	1.536 ± 0.014	PW
RCCSD(T)/CBS[b] [EA_0][c]	[1.543]	PW
UCCSD(T)-F12x/C[d]	1.488, 1.507, 1.415, 1.434, 1.564, 1.463	PW
UCCSD(T)-F12x/D[e]	1.487, 1.506, 1.414, 1.433, 1.563, 1.463	PW
UCCSD(T)-F12b/D [EA_0][f]	[1.494]	PW
UCCSD(T)-F12x/E[g]	1.499, 1.512, 1.417, 1.430, 1.556, 1.474	PW
UCCSD(T)-F12b/E [EA_0][c]	[1.506]	PW
CCSD(T)/AVTZ [EA_0][h]	[1.462]	3
BLYP/DZP++	1.38	1
B3LYP/DZP++	1.53	1
RCCSD(T)/AVQZ	1.51	1
Photodetachment, [EA_0]	$[1.514 \pm 0.010]$	3

[a]PW for present work.
[b]Extrapolation to the complete basis set (CBS) limit using the $1/X^3$ formula with the RCCSD(T)/A and RCCSD(T)/B values. The estimated uncertainty is the difference between the RCCSD(T)/CBS and RCCSD(T)/B values.
[c]ZPE corrections using computed UCCSD(T)-F12b/E harmonic vibrational frequencies.
[d]The given EA values are the UCCSD(T)-F12b, UCCSD(T)-F12a, UCCSD-F12b, UCCSD-F12a, RMP2-F12, and RMP2 values obtained using basis set C at the UCCSD(T)-F12b/C optimized geometries of the neutral and anion.
[e]The given EA values are the UCCSD(T)-F12b, UCCSD(T)-F12a, UCCSD-F12b, UCCSD-F12a, RMP2-F12, and RMP2 values obtained using basis set D at the UCCSD(T)-F12b/D optimized geometries of the neutral and anion.
[f]ZPE corrections using computed UCCSD(T)-F12b/D harmonic vibrational frequencies.
[g]The given EA values are the UCCSD(T)-F12b, UCCSD(T)-F12a, UCCSD-F12b, UCCSD-F12a, RMP2-F12, and RMP2 values obtained using basis set E at the UCCSD(T)-F12b/E optimized geometries of the neutral and anion.
[h]At B3LYP/AVTZ geometries using GAUSSIAN03 [hence UHF/CCSD(T) energy for P_2H]; see original work for detail.

might have slightly overestimated CBS contributions. Nevertheless, a difference of 0.67 kcal mole^{-1} between theory and experiment for the EA_0 value of P_2H is still within a commonly acceptable chemical accuracy of 1 kcal mole^{-1} (0.043 eV).

Regarding results obtained from UCCSD(T)-F12x calculations, UCCSD(T)-F12b, UCCSD(T)-F12a, UCCSD-F12b, UCCSD-F12a, RMP2-F12, and RMP2 EA values were computed and are given in Table IV for comparison. First, similar to the optimized geometrical parameters discussed above, the differences between using basis sets C and D are negligibly small. Second, core contributions (differences between using basis set C or D, where P core electrons were excluded, and basis set E, where P $2s^2 2p^6$ core electrons were explicitly correlated; see Table I) to the computed EA values are ~0.01 eV, similar to the RCCSD(T) results discussed above. Third, the differences in the computed EA values obtained between employing the UCCSD(T)-F12a and UCCSD(T)-F12b methods are 0.019 eV with basis sets C and D, and 0.013 eV with basis set E. In all cases, the F12a values are larger than the F12b values, and slightly closer to the experimental value than the corresponding F12b values. In this connection, with a TZ quality basis set, the F12a method may be preferred to the F12b method as suggested in the MOLPRO user manual.[27] Nevertheless, in general, the differences of below 0.02 eV in the computed relative electronic energy between the two variants of the F12x (x = a or b) method can be considered to be insignificant. Fourth, all the theoretically lower level results (i.e., UCCSD-F12x without triples, RMP2-F12, and RMP2) are either too large or too small by ~0.05 eV, when compared with the UCCSD(T)-F12x values. Finally, it is pleasing that the UCCSD(T)-F12b/E EA_0 value of 1.506 eV agrees very well with the experimental value of 1.514 eV.

Simulated photodetachment spectrum of P_2H^-

The simulated spectra obtained using three different PEFs are compared with the experimental spectrum[3] (taken at the magic angle[38]) in Figure 1. The simulated spectra shown in Figure 1 were obtained employing the equilibrium geometries of the two electronic states as derived from their respective PEFs (see Tables II and III), and a Boltzmann vibrational temperature of 300 K. It can be seen that the three simulated spectra obtained using three different sets of PEFs are essentially identical, suggesting that the three sets of PEFs used are of very similar quality. Therefore, we only consider simulated spectra obtained from one of the three sets of PEFs [UCCSD(T)-F12b/E] from here onwards. When the purely theoretical simulated spectra are compared with the experimental spectrum in Figure 1, it is pleasing to see that the agreement is already reasonably good, particularly for weak spectral features, which will be examined in more detail below.

When the IFCA procedure is carried out to obtain a simulated spectrum, which best matches the experimental spectrum, the following points have been considered. First, the vibrational structure of a photodetachment spectrum carries information only on the magnitudes of changes in the

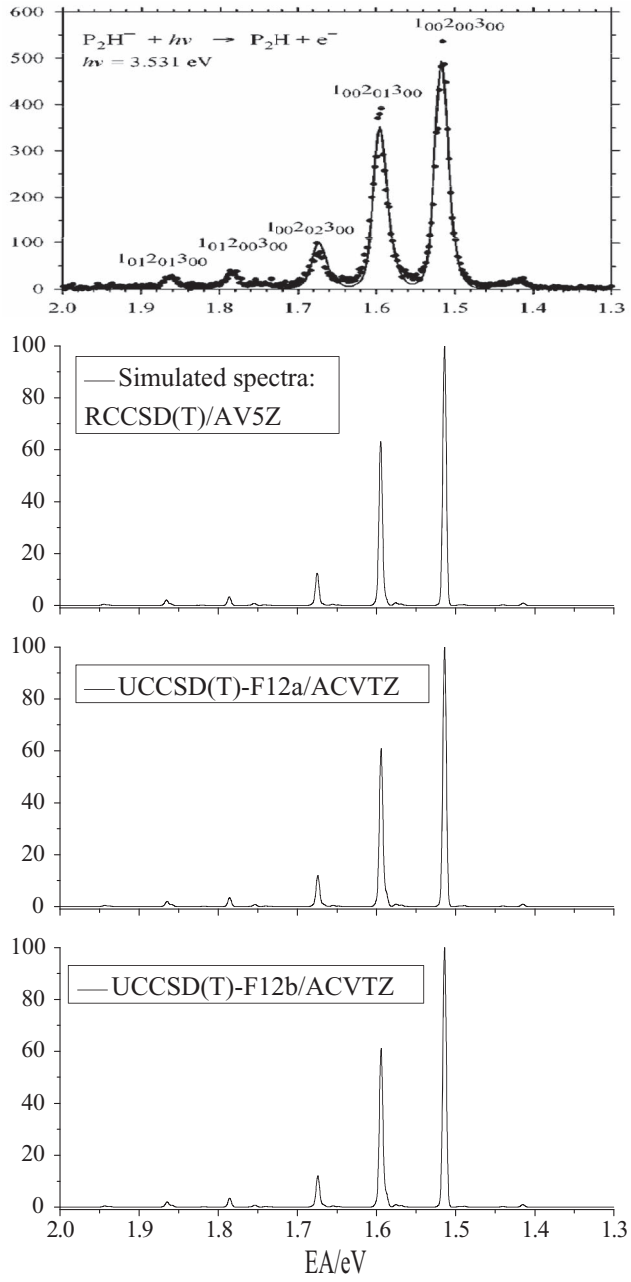

FIG. 1. Comparison between experimental (top trace from Ref. 3) and simulated photodetachment spectra of P_2H^-; the simulated spectra were obtained at a Boltzmann vibrational temperature of 300 K, employing the RCCSD(T)/B1 (second trace from top), UCCSD(T)-F12a/E (second trace from bottom) and UCCSD(T)-F12b/E (bottom trace) PEFs, and the respective computed equilibrium geometries of the two electronic states involved.

equilibrium geometrical parameters of the two electronic states involved upon photodetachment, but not on the direction of the changes and the absolute magnitudes of the geometrical parameters of both states. In this connection, in the IFCA procedure, the geometrical parameters of one state have to be fixed usually to available experimental values, while those of the other state are varied based on the predicted directions of changes from *ab initio* calculations (see, for example, Ref. 37). However, in the present case, experimental geometrical parameters are unavailable for both states concerned. Nevertheless, the best theoretical geometrical parameters obtained in the present study can be used, but the geometry to be fixed can be either that of P_2H or P_2H^-. In this connection, we have carried out IFCA fixing the geometry of either P_2H or P_2H^- to the respective RCCSD(T)/CBS geometry, and obtained two different sets of derived geometries of P_2H and P_2H^- depending on which geometry is fixed in the IFCA procedure (*vide infra*). Nevertheless, as expected, as long as the geometry changes employed are the same, the IFCA procedure gives essentially identical simulated spectra, regardless of which geometry has been fixed. Second, in addition to the IFCA procedure discussed, we have also varied the Boltzmann vibrational temperature to be used in the spectral simulation, particularly for matching the "hot bands." However, there are limitations in the comparison between simulated and experimental spectra and they mainly come from the quality of the experimental spectrum, notably the spectral resolution and the experimental signal-to-noise. Within these experimental restrictions, a best match between the simulated and experimental spectra has been obtained using a Boltzmann temperature of 330 K, with the PP and PH bond lengths being fixed to the RCCSD(T)/CBS values (in the anion or the neutral), and a bond angle change of –9.25° upon photodetachment, regardless of whether the bond angle of P_2H or P_2H^- has been fixed to the RCCSD(T)/CBS values in the IFCA procedure. From the IFCA procedure, it is clear that any further variations in the geometrical parameters and/or the Boltzmann temperature would not be meaningful with the quality of the available experimental spectrum. In any case, the best simulated spectrum, which gives the best overall match with the experimental spectrum, is shown in Figure 2 together with the experimental spectrum. It is pleasing especially to see that the best simulated spectrum thus obtained gives very clear weak features, which match very well those in the experimental spectrum, and these weak spectral features will be discussed below.

Based on the simulated spectrum (Figure 2) and the computed FCFs of the main band (0 K simulated spectrum; Figure 3) and "hot bands" (Figure 4), the assignment of the main experimental vibrational structure given previously[3,4] to the 2_0^n and $1_0^1 2_0^n$ series is confirmed. In addition, all weak spectral features in the experimental spectrum, which are not well resolved and could not be assigned before, can now be assigned with the aid of the simulated spectrum and computed FCFs. Specifically, the very weak features in the 1.4 to 1.5 eV region and on the low electron binding energy shoulders of the main 2_0^0, 2_0^1, and 2_0^2 vibrational components are mainly "hot bands" arising from electron detachment from the (0,0,1) and (0,1,0) vibrational levels of P_2H^- (top and middle bar diagrams in Figure 4). Moreover, although vibrational components due to the PP stretching in P_2H, such as the 3_0^1 vibrational component, have not been identified in the experimental spectrum from previous studies,[3,4] our computed FCFs suggest that they should have appreciable intensities, and in the simulated spectrum (Figure 2) with a resolution of 5 meV FWHM, the 3_0^1 and $2_0^1 3_0^1$ components at 1.588 and 1.668 eV can just be resolved as shoulders at the low electron binding energy side of the 2_0^1 and 2_0^2 peaks at 1.594 and

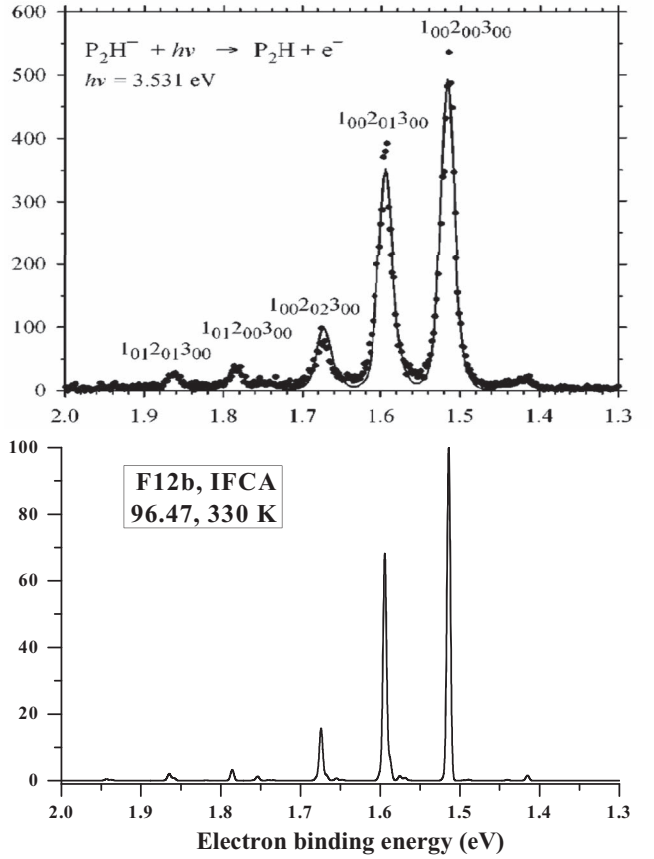

FIG. 2. Comparison between experimental (top trace from Ref. 3) and simulated photodetachment spectra of P_2H^-; the simulated spectrum was obtained at a Boltzmann vibrational temperature of 330 K, employing the UCCSD(T)-F12b/E PEFs and the RCCSD(T)/CBS geometrical parameters of the two electronic states involved, except that the bond angle of P_2H was set to 96.47° in the IFCA procedure (see text).

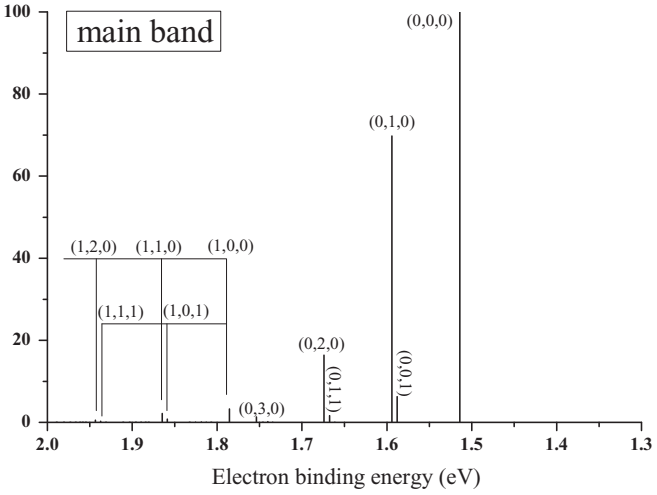

FIG. 3. Computed Franck-Condon factors and vibrational designations, (v_1',v_2',v_3'), of the simulated vibrational structure in the main band of the P_2H $\tilde{X}^2A' + e \leftarrow P_2H^-$ $\tilde{X}^1A'$ (0,0,0) photodetachment spectrum, obtained with the UCCSD(T)-F12b/E PEFs for the two electronic states involved and the IFCA geometries ($\theta_e = 96.47°$ for P_2H; see text and figure caption of Figure 2) at a Boltzmann vibrational temperature of 0 K.

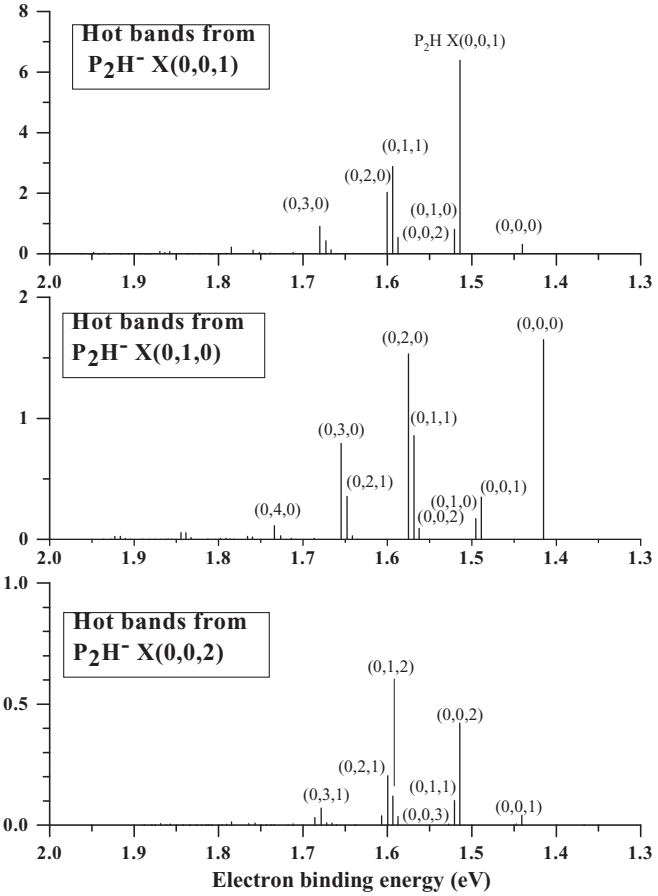

FIG. 4. Computed Franck-Condon factors and vibrational designations, (v_1',v_2',v_3'), of the simulated vibrational structure in some "hot bands" of the P_2H $\tilde{X}^2A' + e \leftarrow P_2H^-$ $\tilde{X}^1A'$ photodetachment spectrum, obtained at 330 K with the UCCSD(T)-F12b/E PEFs for the two electronic states involved and the IFCA geometries ($\theta_e = 96.47°$ for P_2H; see text and figure caption of Figure 2).

1.674 eV, respectively (see also Figure 3). Although Ref. 3 has stated that the resolution of the kinetic-energy analyzer used was 5–8 meV over the entire energy range, the published photodetachment spectrum of P_2H^- suggests a working resolution of probably ~23 meV FWHM, which could not resolve these relatively weak vibrational components of the ν_3', PP stretching mode of P_2H. Computed ν_3' values of P_2H are smaller than computed ν_2' values by ~50 cm^{-1} (6.2 meV; see Table II). In order to resolve vibrational components due to the PP stretching mode from those due to the bending mode, a resolution of at least 5 meV FWHM is required, as shown in the simulated spectrum (Figure 2). However, some weak "hot bands" are so close in energy with the main 2_0^n components that they would not be resolved even with a spectral resolution of 5 meV as used in the simulated spectrum. Nevertheless, most of the vibrational designations of the main band and "hot bands" are given in Figures 3 and 4, including some weak $1_0^1 2_0^n$ and $1_0^1 2_0^n 3_0^1$ combination bands in the 1.78 to 1.95 eV region (Figure 3). Summing up, the present study has provided a much more detailed assignment for the vibrational structure of the photodetachment spectrum of P_2H^- than reported previously.

TABLE V. Computed geometry changes (bond lengths in Angstrom and bond angle in degrees) upon photodetachment of P_2H^- obtained at different levels of calculations.

Methods[a]	Δr_e(PP)	Δr_e(PH)	$\Delta\theta_e$	Remarks	Reference[b]
RCCSD(T)/A2	−0.0189	−0.0283	−8.61	VQZ; frozen P 1*s*2*s*2*p*	PW
RCCSD(T)/B1	−0.0191	−0.0285	−8.60	V5Z; frozen P1*s*2*s*2*p*	PW
RCCSD(T)/B1 PEF	−0.0193	−0.0282	−8.46	V5Z; frozen P1*s*2*s*2*p*	PW
RCCSD(T)/A	−0.0191	−0.0290	−8.69	CVQZ; frozen P1*s*	PW
RCCSD(T)/B	−0.0189	−0.0284	−8.68	CV5Z; frozen P1*s*	PW
RCCSD(T)/CBS	−0.0187	−0.0281	−8.67	CV∞Z; frozen P1*s*	PW
UCCSD(T)-F12a/E PEF	−0.0186	−0.0286	−8.62	CVTZ; frozen P1*s*; F12a	PW
UCCSD(T)-F12b/E PEF	−0.0184	−0.0286	−8.66	CVTZ; frozen P1*s*; F12b	PW
B3LYP/6-311G(2*d*,*p*)	−0.0293	−0.0324	−7.65		4
B3LYP/6-311G(3*df*)	−0.0251	−0.0346	−7.52		4
CCSD/6-311+G(2*d*,*p*)	−0.0138	−0.0325	−8.45		4
B3LYP/DZP++	−0.023	−0.034	−7.7		1
RCCSD(T)/AVTZ	−0.019	−0.029	−8.7		1
RCCSD(T)/AVQZ	−0.020	−0.028	−8.5		1
IFCA[c]	−0.023	−0.068	−8	Harmonic FCF	3
IFCA[d]	−0.026	−0.068	−8.3	Harmonic FCF	4
IFCA[e]	−0.0187	−0.0281	−9.25	Anharmonic FCF, 330 K	PW

[a]See footnotes of Tables II and III.
[b]PW for present work.
[c]The geometrical parameters of the anion were derived from fitting computed Franck-Condon factors to the observed vibrational structure using the B3LYP/AVTZ geometry of the neutral; see original work for detail.
[d]Employing the B3LYP/6-311G(2*d*,*p*) geometry of the neutral to obtain the geometry of the anion; see original work for detail.
[e]The geometrical parameters of the two electronic states were fixed to the RCCSD(T)/CBS values, except for the bond angles (see text).

CONCLUDING REMARKS

We have carried out state-of-the-art *ab initio* calculations on the ground electronic states of P_2H and its anion. In addition to reporting the currently most reliable theoretical geometrical parameters of P_2H and P_2H^-, which have been computed at the RCCSD(T)/CBS level (including P $2s^2 2p^6$ core correlation), we have derived from the photodetachment spectrum of P_2H^-, two sets of geometrical parameters for these two species via the IFCA procedure. While the derived IFCA PP and PH bond lengths are the same as those obtained at the RCCSD(T)/CBS level, the two sets of bond angles for P_2H (P_2H^-) are 96.47° (105.72°) and 97.05° (106.30°), both with a bond angle change of −9.25° upon electron detachment of P_2H^-; the first and second sets have the bond angle of P_2H^- and P_2H fixed to the RCCSD(T)/CBS values, respectively. The differences in the two values obtained for P_2H and P_2H^- are a measure of the uncertainty in the bond angles from the method used. We just note that relativistic and higher order (beyond triple excitations) electron correlation contributions have been ignored in the present study. Nevertheless, for molecules consisting of second row elements (e.g., P in this work), relativistic effects have been found to be negligibly small[39] or have been ignored.[40] Higher order contributions are usually of a similar order of magnitude to that from CBS contributions (∼0.002 Å in bond length and 0.014 eV in EA, as estimated in this work; see, for example, Ref. 40).

Since the vibrational structure in the photodetachment spectrum of P_2H^- carries information on the magnitudes of geometry changes upon electron detachment, we have compiled available computed and experimentally derived (via IFCA) geometry changes in Table V. It can be seen that computed geometry changes at relatively high levels of calculations [CCSD(T) with a large basis set] are fairly consistent for all three geometrical parameters considered, while the bond length and angle changes from DFT calculations are larger and smaller than the CCSD(T) changes, respectively. Regarding the experimentally derived geometry changes via the IFCA procedure, those from Refs. 3 and 4, employing a harmonic model, are similar to each other, but their bond length and angle changes are significantly larger and smaller, respectively, than those obtained in the present investigation which has included anharmonicity. Also, the agreement of the IFCA geometry changes including anharmonicity with the best theoretical RCCSD(T)/CBS geometry changes, both obtained in the present study, is much better than that of the IFCA geometry changes obtained within the harmonic oscillator model from Refs. 3 and 4, especially for the change in the PH bond length upon electron detachment [−0.028 Å from RCCSD(T)/CBS and IFCA including harmonicity versus −0.068 Å from Refs. 3 and 4 without anharmonicity; see Table V]. This is expected, because anharmonicity is particularly important for the PH stretching mode, as mentioned above. Regarding the bond angle change upon electron detachment from P_2H^-, which is the largest change of the three geometrical parameters, although the IFCA change obtained here including anharmonicity is larger than the best theoretical RCCSD(T)/CBS value by 0.58°, it can be concluded that theory and experiment agree reasonably well in the geometry changes upon electron detachment when anharmonicity is included in the theoretical model. The bond angle changes derived from the IFCA procedures within the harmonic model from Refs. 3 and 4 (−8° and −8.3°; Table V) are smaller than the corresponding IFCA value including anharmonicity

(−9.25°) and the best theoretical value (−8.67°) by ∼1.0° and 0.4°, suggesting that anharmonicity is also significant for the bending mode. Summing up, including anharmonicity in the theoretical model used in the present study has clearly improved the agreement between theory and experiment.

We have calculated both RCCSD(T)/AV5Z and UCCSD(T)-F12x (x = a or b)/ACVTZ PEFs for the ground electronic states of P_2H and P_2H^- in the present study, and used them to compute anharmonic vibrational wavefunctions and then FCFs including Duschinsky rotation and anharmonicity. Employing the computed FCFs, we find that simulated photodetachment spectra obtained using these RCCSD(T) and UCCSD(T)-F12x PEFs are almost identical. This once again supports our previous conclusion[11–13] that the explicitly correlated method, UCCSD(T)-F12x, could be used to generate reliable PEFs *in lieu* of conventional correlated methods, such as RCCSD(T), at a considerably reduced cost. In addition, we have reported computed fundamental vibrational frequencies for P_2H and P_2H^- for the first time, and these computed frequencies agree very well with available experimental values from the photodetachment spectrum of P_2H^-. Moreover, our computed FCFs and simulated spectrum have provided a more detailed assignment for the vibrational structure observed in the photodetachment spectrum of P_2H^- than previously reported.

Finally, we have also calculated anharmonic vibrational wavefunctions of P_2D and P_2D^-, and their FCFs, using the UCCSD(T)-F12b/E PEFs. The computed harmonic (fundamental) vibrational frequencies of P_2D are 1651.5 (1597.0), 617.3 (612.3), and 461.9 (458.6) cm^{-1} for the PD and PP stretching modes and the bending mode, respectively. Similarly, for P_2D^-, they are 1463.4 (1390.4), 601.8 (596.3), and 589.3 (580.8) cm^{-1}. It should be noted that, for both P_2D and P_2D^-, the computed PP stretching frequencies (ω_2 and ν_2) are larger than the bending frequencies (ω_3 and ν_3), giving a different order from those of P_2H and P_2H^-. We have also simulated the photodetachment spectrum of P_2D^- (Figure 5), yet to be recorded experimentally. The computed FCFs and vibrational designations of some major vibrational components, including "hot bands," are also given in Figure 5. It can be seen in Figure 5 that, for P_2D, the PP stretching and bending vibrational components are more well separated from each other than in the case of P_2H (Figures 2 and 3), because for P_2D, ν_2' and ν_3' differ by 153.7 cm^{-1} (19 meV). Also, the computed FCFs of the PP stretching mode in the photodetachment of P_2D^- are larger than those in the photodetachment of P_2H^- (see Figures 3 and 5). Based on the computed FCFs and simulated spectrum reported here, the PP stretching progression of P_2D should be identifiable in the experimental photodetachment spectrum of P_2D^-, when it becomes available. In this connection, it will be interesting to see whether theory is ahead of experiment for the photodetachment spectrum of P_2D^-, as was the case of the 351 nm photodetachment spectrum of CCl_2^-.[41,42]

Summarizing, we have carried out state-of-the-art *ab initio* calculations and FCF calculations including anharmonicity on P_2H and P_2H^-. These calculations have contributed to the analysis of the vibrational structure of the photodetachment spectrum of P_2H^-. In addition, we have derived the currently most reliable geometries of P_2H and P_2H^-. Finally, we have simulated the photodetachment spectrum of P_2D^-, which is currently not available experimentally, hoping that this simulated spectrum would stimulate spectroscopists to record the experimental spectrum soon.

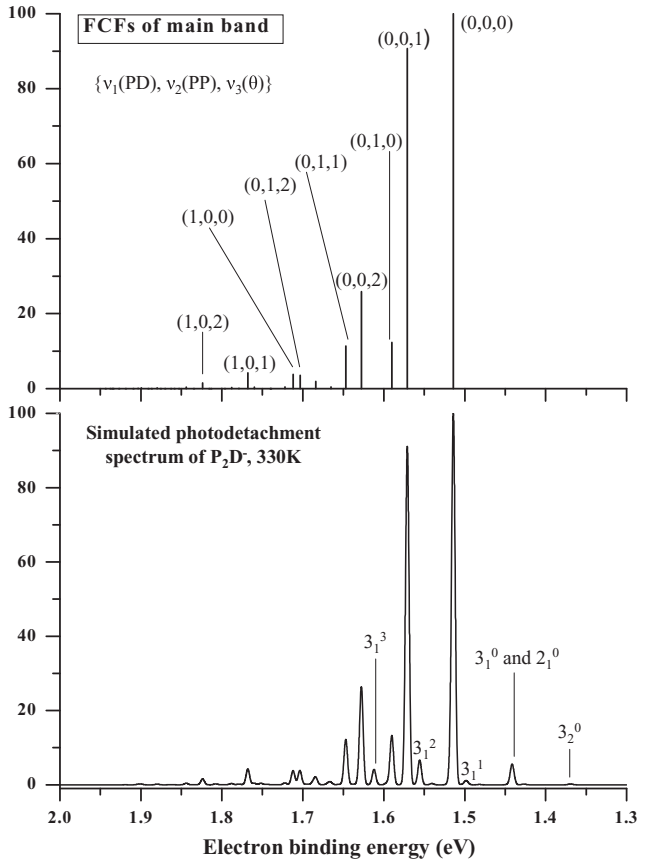

FIG. 5. Computed FCFs of the main band (at 0 K) and simulated photodetachment spectrum of P_2D^- obtained at 330 K employing the UCCSD(T)-F12b/E PEFs for the two electronic states involved and the IFCA geometries ($\theta_e = 96.47°$ for P_2D; see text and figure caption of Figure 2).

ACKNOWLEDGMENTS

Financial support from the Research Grant Council (RGC) of the Hong Kong Special Administrative Region (HKSAR, Grant Nos. PolyU 5003/09P and 5018/09P) is acknowledged. The authors are also grateful to the Research Committee of the Hong Kong Polytechnic University of HKSAR for supports (Grant No. G-YG99), and to the National Service for Computational Chemistry Software (NSCCS) and Engineering and Physical Sciences Research Consul (United Kingdom) [EPSRC (UK)], for the provision of computational resources.

[1] Z. T. Owens, J. D. Larkin, and H. F. Schaefer III, J. Chem. Phys. **125**, 164322 (2006).
[2] M. H. Matus, M. T. Nguyen, and D. A. Dixon, J. Phys. Chem. A **111**, 1726 (2007).
[3] K. M. Ervin and W. C. Lineberger, J. Chem. Phys. **122**, 194303 (2005).
[4] J. Wu, X. Zhang, F. Chen, and Z. Cui, J. Mol. Struct: THEOCHEM **767**, 149 (2006).
[5] M. E. Harding, J. Vázquez, B. Ruscic, A. K. Wilson, J. Gauss, and J. F. Stanton, J. Chem. Phys. **128**, 114111 (2008).

[6]E. F. Valeev and T. D. Crawford, J. Chem. Phys. **128**, 244113 (2008).
[7]G. Czako, B. Nagy, G. Tasi, A. Somogyi, J. Simunek, J. Noga, B. J. Braams, J. M. Bowman, and A. G. Csaszar, Int. J. Quantum Chem. **109**, 2393 (2009).
[8]G. Knizia, T. B. Adler, and H.-J. Werner, J. Chem. Phys. **130**, 054104 (2009).
[9]X. Huang, E. F. Valeev, and T. J. Lee, J. Chem. Phys. **133**, 244108 (2010).
[10]F. Neese and E. F. Valeev, J. Chem. Theory Comput. **7**, 33 (2010).
[11]E. P. F. Lee, D. K. W. Mok, F.-T. Chau, and J. M. Dyke, J. Chem. Phys. **132**, 234309 (2010).
[12]D. K. W. Mok, E. P. F. Lee, F.-T. Chau, and J. M. Dyke, Phys. Chem. Chem. Phys. **132**, 9075 (2010).
[13]D. K. W. Mok, E. P. F. Lee, F.-T. Chau, and J. M. Dyke, J. Comput. Chem. **32**, 1648 (2011).
[14]P. J. Knowles, C. Hampel, and H.-J. Werner, J. Chem. Phys. **99**, 5219 (1993); P. J. Knowles, C. Hampel, and H.-J. Werner Erratum: J. Chem. Phys. **112**, 3106 (2000).
[15]H.-J. Werner, P. J. Knowles, R. Lindh, F. R. Manby, M. Schült *et al.*, MOLPRO, version 2009.1, a package of *ab initio* programs, 2009, see http://www.molpro.net.
[16]T. H. Dunning, Jr., J. Chem. Phys. **90**, 1007 (1989).
[17]D. E. Woon and T. H. Dunning, Jr. J. Chem. Phys. **98**, 1358 (1993).
[18]T. H. Dunning, Jr., K. A. Peterson, and A. K. Wilson, J. Chem. Phys. **114**, 9244 (2001).
[19]K. A. Peterson and T. H. Dunning, Jr., J. Chem. Phys. **117**, 10548 (2002).
[20]K. A. Peterson, T. B. Adler, and H.-J. Werner, J. Chem. Phys. **128**, 084102 (2008).
[21]J. G. Hill, S. Mazumder, and K. A. Peterson, J. Chem. Phys. **132**, 054108 (2010).
[22]K. E. Yousaf and K. A. Peterson, Chem. Phys. Lett. **476**, 303 (2009).
[23]K. E. Yousaf and K. A. Peterson, J. Chem. Phys. **129**, 184108 (2008).
[24]F. Weigend, Phys. Chem. Chem. Phys. **4**, 4285 (2002).
[25]C. Hättig, Phys. Chem. Chem. Phys. **7**, 59 (2005).
[26]F. Weigend, A. Kohn, and C. Hattig, J. Chem. Phys. **116**, 3175 (2002).
[27]See http://www.molpro.net/info/users?portal=user for MOLPRO Users Manual Version 2010.1.
[28]D. Feller, J. Comput. Chem. **17**, 1571 (1996); K. L. Schuchardt, B. T. Didier, T. Elsethagen, L. Sun, V. Gurumoorthi, J. Chase, J. Li, and T. L. Windus, J. Chem. Inf. Model. **47**, 1045 (2007).
[29]T. Helgaker, W. Klopper, H. Koch, and J. Noga, J. Chem. Phys. **106**, 9639 (1997).
[30]A. Halkier, T. Helgaker, W. Klopper, P. Jorgensen, and A. G. Csaszar, Chem. Phys. Lett. **310**, 385 (1999).
[31]C. Puzzarini, J. Phys. Chem. A **113**, 14530 (2009).
[32]D. K. W. Mok, E. P. F. Lee, F.-T. Chau, D. C. Wang, and J. M. Dyke, J. Chem. Phys. **113**, 5791 (2000).
[33]D. K. W. Mok, E. P. F. Lee, F.-T. Chau, and J. M. Dyke, J. Chem. Phys. **120**, 1292 (2004).
[34]D. K. W. Mok, E. P. F. Lee, F.-T. Chau, and J. M. Dyke, J. Chem. Theory Comput. **5**, 565 (2009).
[35]S. Carter and N. C. J. Handy, J. Chem. Phys. **87**, 4294 (1987).
[36]J. K. G. Watson, Mol. Phys. **19**, 465 (1970).
[37]D. K. W. Mok, F.-T. Chau, E. P. F. Lee, and J. M. Dyke, J. Comput. Chem. **31**, 476 (2010).
[38]K. M. Ervin, J. Ho, and W. C. Lineberger, J. Chem. Phys. **91**, 5974 (1989).
[39]A. Yachmenev, S. N. Yurchenko, T. Ribeyre, and W. Thiel, J. Chem. Phys **135**, 074302 (2011).
[40]C. Puzzarini1 and V. Barone, J. Chem. Phys. **133**, 184301 (2010).
[41]S. W. Wren, K. M. Vogelhuber, K. M. Ervin, and W. C. Lineberger, Phys. Chem. Chem. Phys. **11**, 4745 (2009).
[42]J. M. Dyke, E. P. F. Lee, D. K. W. Mok, and F.-T. Chau, ChemPhysChem. **6**, 2046 (2005).